Editors' Suggestion

Shortcuts of Freely Relaxing Systems Using Equilibrium Physical Observables

Isidoro González-Adalid Pemartín,[1] Emanuel Mompó,[2,3] Antonio Lasanta,[4,5,6,*] Víctor Martín-Mayor,[1,7] and Jesús Salas[8,9]

[1]Departamento de Física Teórica, Universidad Complutense, 28040 Madrid, Spain
[2]Departamento de Matemática Aplicada, Grupo de Dinámica No Lineal, Universidad Pontificia Comillas, Alberto Aguilera 25, 28015 Madrid, Spain
[3]Instituto de Investigación Tecnológica (IIT), Universidad Pontificia Comillas, 28015 Madrid, Spain
[4]Departamento de Álgebra, Facultad de Educación, Economía y Tecnología de Ceuta, Universidad de Granada, Cortadura del Valle, s/n, 51001 Ceuta, Spain
[5]Instituto Carlos I de Física Teórica y Computacional, Universidad de Granada, E-18071 Granada, Spain
[6]Nanoparticles Trapping Laboratory, Universidad de Granada, Granada, Spain
[7]Instituto de Biocomputación y Física de Sistemas Complejos (BIFI), 50018 Zaragoza, Spain
[8]Departamento de Matemáticas, Universidad Carlos III de Madrid, 28911 Leganés, Spain
[9]Grupo de Teorías de Campos y Física Estadística, Instituto Gregorio Millán, Universidad Carlos III de Madrid, Unidad Asociada al Instituto de Estructura de la Materia, CSIC, Spain

(Received 8 August 2023; revised 15 November 2023; accepted 18 January 2024; published 15 March 2024)

Many systems, when initially placed far from equilibrium, exhibit surprising behavior in their attempt to equilibrate. Striking examples are the Mpemba effect and the cooling-heating asymmetry. These anomalous behaviors can be exploited to shorten the time needed to cool down (or heat up) a system. Though, a strategy to design these effects in mesoscopic systems is missing. We bring forward a description that allows us to formulate such strategies, and, along the way, makes natural these paradoxical behaviors. In particular, we study the evolution of macroscopic physical observables of systems freely relaxing under the influence of one or two instantaneous thermal quenches. The two crucial ingredients in our approach are timescale separation and a nonmonotonic temperature evolution of an important state function. We argue that both are generic features near a first-order transition. Our theory is exemplified with the one-dimensional Ising model in a magnetic field using analytic results and numerical experiments.

DOI: 10.1103/PhysRevLett.132.117102

Introduction.—Controlling and predicting relaxation processes far from equilibrium is still an open task. In spite of historical advances mostly achieved along the 20th century [1–6], with the exception of some cases in molecular gases [7,8], we lack a general theory beyond the linear response theory and fluctuation theorems allowing us to manage transient regimes and, in particular, optimize relaxation times of a freely evolving system between two desired states [9]. Recent progress unraveling anomalous relaxation processes in out-of-equilibrium systems points in that direction.

An outstanding example is the Mpemba effect (ME) [10–12]. Put instantly two systems—identical but for their different initial temperatures—in contact with a thermal bath at a colder-than-both temperature. The ME happens when the initially hotter system cools faster than the system that was initially closer to equilibrium.

In Markovian systems, the ME can be well understood using a spectral decomposition and diminishing or canceling slow-decaying modes for the sake of enhancing the fast ones. This has been done both in classical [13–20] and open quantum systems [21–23]. Meanwhile, in systems where spectral methods are not applicable, other strategies can be used for controlling fast and slow evolution using macroscopic observables. Namely, energy nonequipartition in water [24], a particular condition in kurtosis in granular gases [25–27], and correlation length in spin glasses [28]. Furthermore, other strategies using several quenches have been shown to be useful in attaining a speedup in relaxation times: preheating protocols [29], taking advantage of magnetic domains growth when a large number of degrees of freedom near phase transitions are present in the system and timescale separation is not possible [30], or different control techniques [31,32].

We shall not overlook that achieving a speedup is not a trivial task. As it has been experimentally shown, the Kovacs effect prevents fast relaxation when using two quenches in a naive way, either for heating or cooling [33–36]. What is even more surprising is that, recently, another anomaly which was verified both theoretically and experimentally has been found: far from equilibrium, there can appear an asymmetry between equidistant and symmetric heating and cooling processes [37,38]. Even more fundamental is that, using reciprocal relaxation processes

between two fixed temperatures, the asymmetry is also found [38]. This has been successfully explained using the so-called "thermal kinematics" [38] based on information geometry [39,40].

Here, we aim to control the out-of-equilibrium evolution of a system *solely* relying on its in-equilibrium physical observables and on the spectral decomposition of the dynamic-generating matrix. Our focus is on observable dynamics: clever computational speedups lacking an experimental counterpart (think, e.g., of Ref. [41]) are excluded. The physical interpretation is straightforward. By identifying the slowest-decaying physical observables, we are able to project the system under study onto the faster ones in order to speed up the total relaxation of the system. Near first order phase transitions, the desired fast relaxation can be achieved choosing the appropriate initial condition, or, previous to the final relaxation, by briefly heating or cooling the system. To showcase this, we use the antiferromagnetic (AF) 1D Ising model with a magnetic field.

Theoretical framework.—We shall model the microscopic dynamics in contact with a thermal bath at temperature T_b through a Markov dynamics with continuous time [42], obtained as the continuous limit of some discrete-time Markov chain (in our case, heat-bath dynamics [43]).

There are two complementary viewpoints on Markov dynamics. Either one considers the time evolution of the probability distribution function (the so-called strong form of the associated stochastic differential equation), or one focuses on the time evolution of observable magnitudes (the weak form) [44]. While the strong form has been emphasized in recent work [32], we shall privilege the very insightful weak-form approach. We briefly recall now the main ingredients of both approaches (see Refs. [42,45] for details).

Let Ω be the set of all possible states of a system [48]. The strong form of the dynamics focus on the master equation for $P_{\boldsymbol{y}}^{(t)}$, the probability of finding the system in the microscopic state $\boldsymbol{y}$ at time t:

$$\frac{dP_{\boldsymbol{y}}^{(t)}}{dt} = \frac{1}{\tau_0}\sum_{\boldsymbol{x}\in\Omega} P_{\boldsymbol{x}}^{(t)} R_{\boldsymbol{x},\boldsymbol{y}}, \tag{1}$$

where $R_{\boldsymbol{x},\boldsymbol{y}}/\tau_0$ is the probability per unit time for the system to jump from state $\boldsymbol{x}$ to state $\boldsymbol{y}$ when subject to a thermal bath with temperature T_{b} (τ_0 is a fixed time unit). Setting the diagonal term as $R_{\boldsymbol{x},\boldsymbol{x}} = -\sum_{\boldsymbol{y}\in\Omega\setminus\{\boldsymbol{x}\}} R_{\boldsymbol{x},\boldsymbol{y}}$ ensures the conservation of the total probability. The master equation can be solved by expressing the initial probability $\boldsymbol{P}^{(t=0)}$ as a linear combination of the left eigenvectors of the matrix R (see, e.g., [42,45]), but this would take us too far off field. Instead, we wish to focus on the weak form of the dynamics, for which there are two crucial mathematical ingredients.

Our first ingredient is the inner product between two observables, $\mathcal{A}$ and $\mathcal{B}$ (i.e., two mappings from Ω to the real numbers). Let $\mathbb{E}^T[\mathcal{A}] = \sum_{\boldsymbol{x}\in\Omega} \pi_{\boldsymbol{x}}^T \mathcal{A}(\boldsymbol{x})$ be the equilibrium expected value of $\mathcal{A}$ at temperature T ($\pi_{\boldsymbol{x}}^T$ is the Boltzmann weight for state $\boldsymbol{x}$). The inner product of $\mathcal{A}$ and $\mathcal{B}$ is defined at the bath temperature:

$$\langle \mathcal{A}|\mathcal{B}\rangle := \mathbb{E}^{T_b}[\mathcal{A}\mathcal{B}] = \sum_{\boldsymbol{x}\in\Omega} \pi_{\boldsymbol{x}}^{T_b} \mathcal{A}(\boldsymbol{x})\mathcal{B}(\boldsymbol{x}). \tag{2}$$

In particular, let $\mathbf{1}$ be the constant observable such that $\mathbf{1}(\boldsymbol{x}) = 1$ for any state $\boldsymbol{x}$. Hence, for any observable $\mathcal{A}$, $\langle \mathbf{1}|\mathcal{A}\rangle = \mathbb{E}^{T_b}[\mathcal{A}]$, while the equilibrium variance at temperature T_b is $\langle \mathcal{A}^\perp|\mathcal{A}^\perp\rangle$, where $\mathcal{A}^\perp := \mathcal{A} - \mathbf{1}\mathbb{E}^{T_b}[\mathcal{A}]$ accounts for the *fluctuations* of $\mathcal{A}$ from its expected value at T_b. Furthermore, the fluctuation-dissipation theorem tells us that

$$T^2 \left.\frac{d\mathbb{E}^T[\mathcal{A}]}{dT}\right|_{T=T_b} = \langle \mathcal{A}^\perp|\mathcal{E}\rangle \tag{3}$$

($\mathcal{E}$ is the energy, and $\langle \mathcal{A}^\perp|\mathcal{E}\rangle = \mathbb{E}^T[\mathcal{A}\mathcal{E}] - \mathbb{E}^T[\mathcal{A}]\mathbb{E}^T[\mathcal{E}]$).

Our second crucial ingredient is the operator $\mathcal{R}$, that generates the time evolution of observables: $\mathcal{R}[\mathcal{A}](\boldsymbol{x}) = \sum_{\boldsymbol{y}\in\Omega} R_{\boldsymbol{x},\boldsymbol{y}}\mathcal{A}(\boldsymbol{y})$ [the matrix R was defined in Eq. (1)]. In particular, $\mathcal{R}[\mathbf{1}](\boldsymbol{x}) = 0$ for all $\boldsymbol{x}$ due to probability conservation (hence, $\mathbf{1}$ is an eigenfunction: $\mathcal{R}[\mathbf{1}] = 0\cdot\mathbf{1}$).

Detailed balance implies that $\mathcal{R}$ is self-adjoint with respect to the inner product (2). For any $\mathcal{A}$ and $\mathcal{B}$

$$\langle \mathcal{R}[\mathcal{A}]|\mathcal{B}\rangle = \langle \mathcal{A}|\mathcal{R}[\mathcal{B}]\rangle. \tag{4}$$

It follows that we can find an orthonormal basis of the space of observables with finite variance $(\mathbf{1}, \mathcal{O}_2^b, \mathcal{O}_3^b, \ldots)$, in which the $\mathcal{O}_k^b$ are all eigenfunctions $\mathcal{R}[\mathcal{O}_k^b] = \lambda_k \mathcal{O}_k^b$ [49]. We order the basis in such a way that $0 = \lambda_1 > \lambda_2 \geq \lambda_3 \geq \ldots$. Take now an arbitrary starting distribution function $\boldsymbol{P}^{(t=0)}$ at time $t = 0$. The expected value of *any* finite-variance observable $\mathcal{A}$ at time $t > 0$ is

$$\mathbb{E}_t[\mathcal{A}] = \mathbb{E}^{T_b}[\mathcal{A}] + \sum_{k\geq 2} \alpha_k^{(t=0)} \beta_k^{\mathcal{A}} \mathrm{e}^{-|\lambda_k|t/\tau_0}, \tag{5}$$

$$\beta_k^{\mathcal{A}} = \langle \mathcal{O}_k^b|\mathcal{A}\rangle, \qquad \alpha_k^{(t=0)} = \sum_{\boldsymbol{x}\in\Omega} P_{\boldsymbol{x}}^{(t=0)} \mathcal{O}_k^b(\boldsymbol{x}). \tag{6}$$

As long as the system shows separation of timescales (i.e., $|\lambda_2| < |\lambda_3|$), Eq. (5) gives rise to a hierarchy of physical magnitudes, with $\mathcal{O}_2^b$ having the slowest decay. If we are able to find an initial setup such that $\alpha_2^{(t=0)} = 0$—all $\alpha_k^{(t=0)}$ are independent of the observable $\mathcal{A}$ under consideration—then, provided that $\beta_2^{\mathcal{A}} \neq 0$, its expected value will benefit from an exponential speedup in the evolution toward its equilibrium value $\mathbb{E}^{T_b}[\mathcal{A}]$.

It is important to notice that the initial setup that will be used to speed up the system—coded in the starting probability $\boldsymbol{P}^{(t=0)}$—is not restricted to an equilibrium state. However, our interest lies on equilibrium states because they are easier to control (e.g., experimentally). For instance, using an equilibrium initial condition, the requirement for a speedup would be met if we can find a temperature $T \neq T_b$ such that $\alpha_2^{(t=0)} \equiv \mathbb{E}^T[\mathcal{O}_2^b] = 0$. We show below how to find (or force) this condition, explaining along the way different anomalous behaviors.

Experimental suitability.—If the number of states is large enough, the spectral decomposition (5) might not be practical. In particular, the slowest decaying observable $\mathcal{O}_2^b$ might be unknown (or, even if known, its experimental measurement may present difficulties). Nonetheless, in some situations there may be a simple way out.

Specifically, let us consider the neighborhood of a first-order phase transition at zero temperature separating two ground states with different symmetries (we consider a specific example below). Let $\mathcal{M}_w$ be the order parameter of the unstable phase (the suffix w stands for *wrong*). If symmetries are such that $\mathbb{E}^T[\mathcal{M}_w] = 0$ for all T, then there are good chances that $(\mathcal{M}_w^2)^\perp$ will be a nice proxy for $\mathcal{O}_2^b$. Indeed, at phase coexistence, slow observable dynamics (OD) often stems from metastability [50]. We consider $(\mathcal{M}_w^2)^\perp$, the fluctuating part of $\mathcal{M}_w^2$, to mimic the behavior of $\mathcal{O}_2^b$: $0 = \langle \mathbf{1}|\mathcal{O}_2^b\rangle = \mathbb{E}^{T_b}[\mathcal{O}_2^b]$.

We expect $1 \approx \langle(\mathcal{M}_w^2)^\perp|\mathcal{O}_2^b\rangle / \langle(\mathcal{M}_w^2)^\perp|(\mathcal{M}_w^2)^\perp\rangle^{1/2}$ for any good proxy: in geometrical terms, the angle between $\mathcal{O}_2^b$ and $(\mathcal{M}_w^2)^\perp$ defined by the scalar product (2) will be small.

The crucial point leading to unconventional OD effects is that $\mathbb{E}^T[\mathcal{M}_w^2]$ is a nonmonotonic function of T, and we can find a bath temperature T_b^* such that $d\mathbb{E}^T[\mathcal{M}_w^2]/dT|_{T=T_b^*} = 0$ (see Figs. 1 and 2). This maximum generates surprising OD.

The behavior in Figs. 1 and 2 is generic because $\mathbb{E}^T[\mathcal{M}_w^2]$ is proportional to the susceptibility of $\mathcal{M}_w$ with respect to its conjugate field. Now, this susceptibility vanishes when $T \to 0$ (because $\mathcal{M}_w$ is the order parameter for the unstable phase) while, for large enough T, all susceptibilities decrease as T grows.

The basic observation.—Consider the spectral decomposition (5) when the starting distribution $\boldsymbol{P}^{(t=0)}$ is the Boltzmann weight for some temperature $T^* \neq T_b$. We can approximate coefficient $\alpha_2^{(t=0)}$ as

$$\alpha_2^{(t=0)} \approx \frac{1}{\Lambda}\left(\mathbb{E}^{T^*}[\mathcal{M}_w^2] - \mathbb{E}^{T_b}[\mathcal{M}_w^2]\right), \tag{7}$$

with $\Lambda = \langle(\mathcal{M}_w^2)^\perp|(\mathcal{M}_w^2)^\perp\rangle^{1/2}$ a relatively uninteresting constant fixed by the bath temperature [51]. In the more general case, $\mathbb{E}^{T^*}[\mathcal{M}_w^2]$ should be traded with $\mathbb{E}_{t=0}[\mathcal{M}_w^2]$ in Eq. (7). Several anomalous effects can be better understood from this simple observation.

The Markovian Mpemba effect [13].—Consider a bath at temperature T_b and two other temperatures, T_c and T_h such that $T_b < T_b < T_h$, chosen to have expected values of $\mathcal{M}_w^2$ as shown in Fig. 1(a). In the view of Eq. (7), it is clear that $\alpha_2^h = 0$, while $|\alpha_2^c| > 0$. This means that, provided that we start from a system in equilibrium at T_h, any observable $\mathcal{A}$ with $\beta_2^{\mathcal{A}} \neq 0$ [cf. Eq. (5)] will benefit from an exponential OD speedup, in its approach to equilibrium at T_b. Instead, the system originally in equilibrium at T_c will display a slower relaxation in the bath at T_b. This is regarded as the strong ME [14]. Mind that, in general, T_h will not be such that $\mathbb{E}^{T_h}[\mathcal{M}_w^2]$ exactly equals $\mathbb{E}^{T_b}[\mathcal{M}_w^2]$, but T_h will be near the temperature where exact equality is achieved. That is, the condition $0 < |\alpha_2^h| < |\alpha_2^c|$ is fulfilled, which leads to a subexponential speedup regarded as the weak ME [14].

In particular, the ME will be most spectacular if we choose $\mathcal{A}$ such that $\mathbb{E}^{T_c}[\mathcal{A}]$ is closer to $\mathbb{E}^{T_b}[\mathcal{A}]$ than $\mathbb{E}^{T_h}[\mathcal{A}]$ is, because in that case the difference $\mathbb{E}_t^h[\mathcal{A}] - \mathbb{E}_t^c[\mathcal{A}]$ will change sign in a clearer way.

Preheating for faster cooling.—In these protocols [29,30] the transition of the system from equilibrium at temperature T_0 toward equilibrium at bath temperature $T_b < T_0$ can be done faster by introducing a brief sudden quench at a higher temperature $T_q > T_0$, rather than simply leaving the system to freely relax under the action of the bath.

In order to amplify the effect, we choose T_0 near the maximum of $\mathbb{E}^T[\mathcal{M}_w^2]$, so that $\alpha_2^{T_0 \to T_b}$ will be as large as possible, cf. Eq. (7). On the other hand, we choose

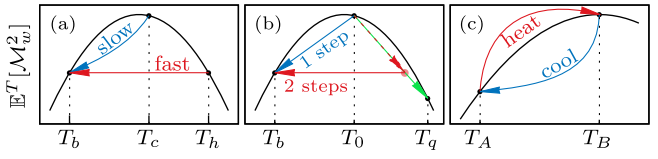

FIG. 1. Staging the anomalous effects. (a) The Mpemba effect. (b) Preheating for faster cooling. (c) Asymmetry of heating and cooling processes.

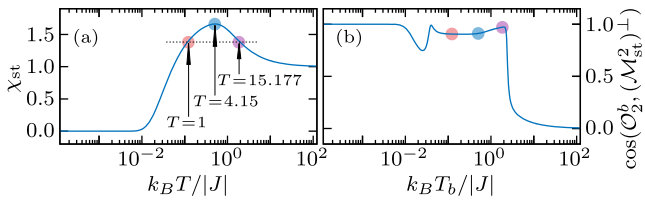

FIG. 2. Validation of $(M_{st}^2)^\perp$ as a proxy for the slowest decaying observable $\mathcal{O}_2^b$. (a) χ_{st} as computed for $N \to \infty$ vs $k_BT/|J|$, see Eq. (10), has a maximum at $T_b^* \approx 4.15$. The curves for $N = 8$ and $N \to \infty$ are hardly distinguishable at this scale. (b) For $N = 8$, the cosine of the angle between $(\mathcal{M}_{st}^2)^\perp$ and $\mathcal{O}_2^b$ is close to 1 for a wide range of bath temperatures. The colored dots in (a) and (b) indicate the three temperatures that we mostly use to demonstrate unconventional OD.

$T_q \gg T_0$ so that $\mathbb{E}^{T_b}[\mathcal{M}_w^2] > \mathbb{E}^{T_q}[\mathcal{M}_w^2]$, see Fig. 1(b). Now, starting from the equilibrated system at T_0, we instantaneously raise the bath temperature to T_q, and let the system relax. During the relaxation, the expected value of $\mathcal{M}_w^2$ decreases from its initial value (which is the T_0 equilibrium value) and eventually crosses $\mathbb{E}^{T_b}[\mathcal{M}_w^2]$ at a time t'. This means [cf. Eq. (7)] that we can find a suitable time $t_w \approx t'$ such that, if we instantaneously lower the bath temperature from T_q to T_b at time t_w, we shall start the relaxation at T_b with $\alpha_2^{t_w} = 0$. The t_w time overhead, due to the initial temperature excursion from T_0 to T_q, is compensated by the exponential speedup at T_b, that would otherwise be absent.

Heating and cooling may be asymmetric processes (see also [37,38]).—Let us consider the maximum of $\mathbb{E}^T[\mathcal{M}_w^2]$ at $T = T_b^*$ in Fig. 1(c). Given the aforementioned relation between metastability and slow relaxations, it is natural to expect that the largest relaxation time in the system $1/|\lambda_2|$, see Eq. (5), will also attain its maximum value at T_b^* (the asymmetry stems from λ_2, rather than α_2). Now, one would naively think taking to equilibrium at T_A a system initially at equilibrium at T_B would take the same time as the inverse process $T_A \to T_B$. Quite on the contrary, if we choose $T_B = T_b^*$ the process $T_B \to T_A$ is *faster* than its counterpart $T_A \to T_B$, no matter whether $T_A < T_B$ or $T_A > T_B$. Indeed, Eq. (7) tells us that $\alpha_2^{T_B \to T_A}$ and $\alpha_2^{T_A \to T_B}$ are numbers of similar magnitude (but opposite sign). Hence, the slowness of the relaxation is ruled by $1/|\lambda_2|$, which is larger at T_B.

The relaxation of the energy is an important exception, however. Indeed, applying Eq. (3) to $\mathcal{M}_w^2$, one finds that $\beta_2^{\mathcal{E}}$ [cf. Eq. (5)] is inordinately small at $T_B = T_b^*$. Therefore, the approach to equilibrium of $\mathcal{E}$ at T_B is ruled by λ_3 rather than λ_2, which precludes us from making definite predictions.

A working example: The antiferromagnetic 1D Ising model.—We consider a periodic chain with N spins $\sigma_i = \pm 1$, $1 \le i \le N$, and $\sigma_{N+1} := \sigma_1$. The state space is given by $\Omega = \{-1, 1\}^N$. The energy for a given spin configuration $\boldsymbol{x} = (\sigma_1, \sigma_2, \ldots, \sigma_N)$ is

$$\mathcal{E}(\boldsymbol{x}) := -J \sum_{k=1}^{N} \sigma_k \sigma_{k+1} - h \sum_{k=1}^{N} \sigma_k, \tag{8}$$

where we assume $J < 0$ and $h > 0$, as well as N even to avoid frustration. The minimum energy configuration differs at both sides of the line $2J + h = 0$. If $J > -h/2$ the ground state (GS) is the uniform configuration $\{\sigma_i = 1\}$. Instead, if $J < -h/2$ the GS is one of the two AF ordered staggered configurations $\{\sigma_i = (-1)^i\}$ or $\{\sigma_i = (-1)^{i+1}\}$. Therefore, the first-order transition at $T = 0$ needed to demonstrate exotic OD is realized in this model.

The uniform ($\mathcal{M}_u$) and the staggered ($\mathcal{M}_{\rm st}$) magnetizations are order parameters able to discriminate our GS:

$$\mathcal{M}_u(\boldsymbol{x}) = \sum_{k=1}^{N} \sigma_k, \qquad \mathcal{M}_{\rm st}(\boldsymbol{x}) = \sum_{k=1}^{N} (-1)^k \sigma_k \tag{9}$$

(for the uniform GS, $\mathcal{M}_u = N$ and $\mathcal{M}_{\rm st} = 0$, while for the staggered GSs one finds $\mathcal{M}_u = 0$ and $\mathcal{M}_{\rm st} = \pm N$). The energy $\mathcal{E}$ (8) is invariant under spatial translations ($\sigma_i \to \sigma_{i+1}$) which ensures that $\mathbb{E}^T[\mathcal{M}_{\rm st}] = 0$ for all temperatures. This is why we make stable the uniform GS by choosing $(J, h) = (-4, 8.2)$. Hence, our *wrong* order parameter will be $\mathcal{M}_w \equiv \mathcal{M}_{\rm st}$.

Other magnitudes of interest will be the staggered susceptibility $\chi_{\rm st}$ and the spin-spin interaction $\mathcal{C}_1$:

$$\chi_{\rm st} = \frac{1}{N} \mathbb{E}^T[\mathcal{M}_{\rm st}^2], \qquad \mathcal{C}_1(\boldsymbol{x}) = \sum_{k=1}^{N} \sigma_k \sigma_{k+1}. \tag{10}$$

The reader will note that all our magnitudes of interest (namely, $\mathcal{M}_u, \mathcal{M}_{\rm st}^2, \mathcal{E}$, and $\mathcal{C}_1$) are invariant under spatial translations. Also our dynamics, see Eq. (1), preserves the translation invariance of the starting probability $\boldsymbol{P}^{(t=0)}$. Hence, the spectral decomposition (5) can be restricted to the subspace of magnitudes $\mathcal{O}_k^b$ that are themselves invariant under translations.

Figure 2 shows that the two conditions necessary for exotic OD [namely, a nonmonotonic behavior of $\chi_{\rm st}$ and a small angle—as defined by Eq. (2)—between $(\mathcal{M}_{\rm st}^2)^\perp$ and $\mathcal{O}_2^b$] are met with our working parameters.

Results.—We have considered the three protocols explained in Fig. 1 in the 1D AF Ising model considered above. We have studied a single-site dynamics (heat-bath dynamics or Gibbs sampler [42,43,45]). For short chains ($N = 8$, 12), we solved the master equation (1) through Monte Carlo (MC) simulations, and by finding the "exact" spectral decomposition of the operator R [52], full details can be found in [45]. The two methods were in full agreement and supported the proposed approach for small $N = 8$, 12. For larger chains ($N = 32$), only MC simulations were computationally feasible and, again, validated our proposal. For clarity's sake, we only show numerical results for a selection observables (see Ref. [45] for the

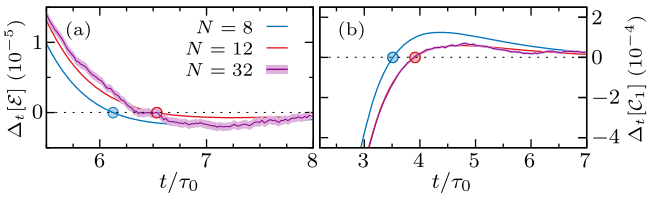

FIG. 3. Mpemba effect. Evolution of $\Delta_t[\mathcal{A}]$ [cf. Eq. (11)] for the observables $\mathcal{A} = \mathcal{E}$ (a) and $\mathcal{A} = \mathcal{C}_1$ (b). We show the results for $N = 8$ (blue), $N = 12$ (red), and $N = 32$ (purple, with a lighter shade representing the error bars of the MC data). The time at which $\Delta_t[\mathcal{A}]$ changes sign is marked by a dot.

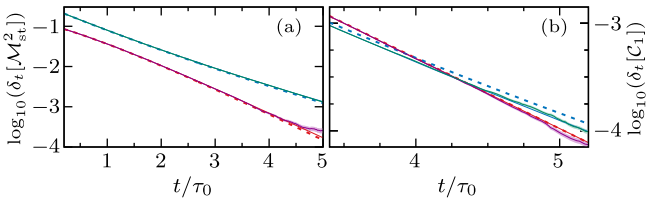

FIG. 4. Preheating strategy for faster cooling. Evolution of $\delta_t[\mathcal{A}]$ [cf. Eq. (12)] for $\mathcal{A} = \mathcal{M}_{\rm st}^2$ (a), and $\mathcal{A} = \mathcal{C}_1$ (b). Colors red and purple (respectively, blue and green) denote that the protocol includes (respectively, does not include) an initial quench at temperature T_q. We show data for $N = 8$ (dashed lines), $N = 12$ (solid lines), and $N = 32$ (solid lines with a lighter shade representing the error bars of the MC data). Both panels show the expected speedup for the preheating protocol.

remaining ones). In all three protocols, we have found statistically compatible results for $N = 12$ and 32.

Figure 3 illustrates the ME as obtained with $T_b = 1$, $T_c = 4.15$, and $T_h = 15.177$, by a change of sign in

$$\Delta_t[\mathcal{A}] := \frac{1}{N}(\mathbb{E}_t^h[\mathcal{A}] - \mathbb{E}_t^c[\mathcal{A}]). \tag{11}$$

Supercooling through preheating is illustrated in Fig. 4, with the choices $T_b = 1$, $T_0 = 4.15$, $T_q = 2000$, and $t_w = 0.156$. It is useful to define

$$\delta_t[\mathcal{A}] := \frac{1}{N}|\mathbb{E}_t[\mathcal{A}] - \mathbb{E}^{T_b}[\mathcal{A}]|. \tag{12}$$

Finally, the asymmetry between heating and cooling is illustrated in Fig. 5(a) with the choices $T_A = 1$ and $T_B = 4.15 \approx T_b^*$, and in Fig. 5(b) with the choices $T_A = 15.177$ and $T_B = 4.15$.

Discussion.—We have shown that the "weak form" of Markov dynamics provides a unified, geometric framework that allows us to explain and control several exotic OD effects pertaining to the Mpemba effect realm. Our approach

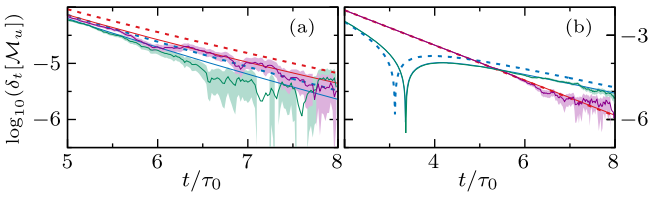

FIG. 5. (A)symmetry in heating and cooling. Evolution of $\delta_t[\mathcal{M}_u]$ [cf. Eq. (12)] for cooling (blue and green) and heating (red and purple) processes. We show data for $N = 8$ (dashed lines), $N = 12$ (solid lines), and $N = 32$ (solid lines with a lighter shade representing the errors of the MC data). The cooling and heating processes were carried out between (a) $T_A = 1$ and $T_B = 4.15$; and (b) $T_A = 15.177$ and $T_B = 4.15$. Note that in panel (b), $\mathbb{E}_t[\mathcal{M}_u] - \mathbb{E}^{T_b=T_B}[\mathcal{M}_u]$ changes sign at $t \approx 3$ for the system originally at $T_A = 15.177$. It is always slower to approach $T_B = 4.15$: i.e., to heat up in (a), and to cool down in (b).

departs from previous work that usually privilege the "strong form" of the dynamics by following the evolution of the system entropy (or, rather, some kind of entropic "distance" such as the Kullback-Leibler divergence [53]). We have dealt, instead, with different physical observables, some of which can be measured at the mesoscopic level. Our geometric approach has unearthed an orthogonality phenomenon that may cause an observable as prominent as the energy to remain blind to the overall speedup achieved by the temperature changing protocols. This result warns that one cannot have a too-narrow spectrum of observables when investigating the Mpemba effect [54,55].

Finite-size effects on the separation of timescales are also of concern, because it is this separation what determines the attainable exponential speedup. Fortunately, we have found that the speedup depends very mildly (if at all) on the system size. Finally, we stress that the approach presented here can also be applied to other systems where anomalous relaxation has been observed [15,29,38], and where the nonmonotonicity of equilibrium thermodynamic observables is also present. Also, extending our approach to the analysis of the time-varying temperature protocols followed in recent experiments [56] is an exciting venue for future work.

We thank Oren Raz for discussions about the nonmonotonic behavior of the susceptibilities with temperature. We also thank Lamberto Rondoni for comments and for pointing out Refs. [7,8]. This work was partially supported by Grants No. PID2022-136374NB-C21, No. PID2021-128970OA-I00, No. PID2020–116567 GB-C22, No. FIS2017-84440-C2-2-P, and No. MTM2017-84446-C2-2-R funded by Ministerio de Ciencia e Innovación y Agencia Estatal de Investigación 10.13039/501100011033, by "ERDF A way of making Europe," and by the European Union. A. L. was also partly supported by FEDER/Junta de Andalucía Consejería de Universidad, Investigación e Innovación, and by the European Union, through Grants No. A-FQM-644-UGR20, and No. C-EXP-251-UGR23. J. S. was also partly supported by the Madrid Government (Comunidad de Madrid-Spain) under the Multiannual Agreement with UC3M in the line of Excellence of University Professors (EPUC3M23), and in the context of the V PRICIT (Regional Programme of Research and Technological Innovation). I. G.-A. P. was supported by the Ministerio de Ciencia, Innovación y Universidades (MCIU, Spain) through FPU Grant No. FPU18/02665. We are also grateful for the computational resources and assistance provided by PROTEUS, the supercomputing center of the Institute Carlos I for Theoretical and Computational Physics at University of Granada, Spain.

*Corresponding author: alasanta@ugr.es

[1] H. Nyquist, Phys. Rev. **32**, 110 (1928).
[2] R. Zwanzig, Annu. Rev. Phys. Chem. **16**, 67 (1965).

[3] L. Onsager, Phys. Rev. **37**, 405 (1931).
[4] L. Onsager, Phys. Rev. **38**, 2265 (1931).
[5] R. Kubo, Rep. Prog. Phys. **29**, 255 (1966).
[6] U. M. B. Marconi, A. Puglisi, L. Rondoni, and A. Vulpiani, Phys. Rep. **461**, 111 (2008).
[7] D. J. Evans, D. J. Searles, and S. R. Williams, J. Chem. Phys. **128**, 014504 (2008).
[8] D. J. Evans, D. J. Searles, and S. R. Williams, J. Chem. Phys. **128**, 249901 (2008).
[9] U. Seifert, Rep. Prog. Phys. **75**, 126001 (2012).
[10] M. Jeng, Am. J. Phys. **74**, 514 (2006).
[11] E. B. Mpemba and D. G. Osborne, Phys. Educ. **4**, 172 (1969).
[12] J. Bechhoefer, A. Kumar, and R. Chétrite, Nat. Rev. Phys. **3**, 534 (2021).
[13] Z. Lu and O. Raz, Proc. Natl. Acad. Sci. U.S.A. **114**, 5083 (2017).
[14] I. Klich, O. Raz, O. Hirschberg, and M. Vucelja, Phys. Rev. X **9**, 021060 (2019).
[15] A. Kumar and J. Bechhoefer, Nature (London) **584**, 64 (2020).
[16] M. R. Walker and M. Vucelja, J. Stat. Mech. (2021) 113105.
[17] A. Biswas, R. Rajesh, and A. Pal, J. Chem. Phys. **159**, 044120 (2023).
[18] F. J. Schwarzendahl and H. Löwen, Phys. Rev. Lett. **129**, 138002 (2022).
[19] A. Kumar, R. Chétrite, and J. Bechhoefer, Proc. Natl. Acad. Sci. U.S.A. **119**, 2118484119 (2022).
[20] N. Vadakkayil and S. K. Das, Phys. Chem. Chem. Phys. **23**, 11186 (2021).
[21] F. Carollo, A. Lasanta, and I. Lesanovsky, Phys. Rev. Lett. **127**, 060401 (2021).
[22] A. Nava and M. Fabrizio, Phys. Rev. B **100**, 125102 (2019).
[23] A. K. Chatterjee, S. Takada, and H. Hayakawa, Phys. Rev. Lett. **131**, 080402 (2023).
[24] A. Gijón, A. Lasanta, and E. R. Hernández, Phys. Rev. E **100**, 032103 (2019).
[25] A. Lasanta, F. Vega Reyes, A. Prados, and A. Santos, Phys. Rev. Lett. **119**, 148001 (2017).
[26] A. Torrente, M. A. López-Castaño, A. Lasanta, F. Vega Reyes, A. Prados, and A. Santos, Phys. Rev. E **99**, 060901(R) (2019).
[27] E. Mompó, M. A. López-Castaño, A. Lasanta, F. Vega Reyes, and A. Torrente, Phys. Fluids **33**, 062005 (2021).
[28] M. Baity-Jesi *et al.*, Proc. Natl. Acad. Sci. U.S.A. **116**, 15350 (2019).
[29] A. Gal and O. Raz, Phys. Rev. Lett. **124**, 060602 (2020).
[30] I. G.-A. Pemartín, E. Mompó, A. Lasanta, V. Martín-Mayor, and J. Salas, Phys. Rev. E **104**, 044114 (2021).
[31] D. Guéry-Odelin, C. Jarzynski, C. A. Plata, A. Prados, and E. Trizac, Rep. Prog. Phys. **86**, 035902 (2023).
[32] S. S. Chittari and Z. Lu, J. Chem. Phys. **159**, 084106 (2023).
[33] A. J. Kovacs, Fortschr. Hochpolym. Forsch. **3**, 394 (1964).
[34] A. J. Kovacs, J. J. Aklonis, J. M. Hutchinson, and A. R. Ramos, J. Polym. Sci. Pol. Phys. **17**, 1097 (1979).
[35] A. Prados and E. Trizac, Phys. Rev. Lett. **112**, 198001 (2014).
[36] A. Militaru, A. Lasanta, M. Frimmer, L. L. Bonilla, L. Novotny, and R. A. Rica, Phys. Rev. Lett. **127**, 130603 (2021).
[37] A. Lapolla and A. Godec, Phys. Rev. Lett. **125**, 110602 (2020).
[38] M. Ibáñez, C. Dieball, A. Lasanta, A. Godec, and R. A. Rica, arXiv:2302.09061.
[39] G. E. Crooks, Phys. Rev. Lett. **99**, 100602 (2007).
[40] S. Ito and A. Dechant, Phys. Rev. X **10**, 021056 (2020).
[41] U. Wolff, Phys. Rev. Lett. **62**, 361 (1989).
[42] D. A. Levin and Y. Peres, *Markov Chains and Mixing Times* (American Mathematical Soc., Providence, 2017), Vol. 107.
[43] A. D. Sokal, *In Functional Integration: Basics and Applications (1996 Cargèse School)*, edited by C. DeWitt-Morette, P. Cartier, and A. Folacci (Plenum, New York, 1997).
[44] These two viewpoints remind the Heisenberg and Schrödinger pictures of time evolution in quantum mechanics.
[45] See Supplemental Material at http://link.aps.org/supplemental/10.1103/PhysRevLett.132.117102 for a short description of the weak and strong forms of Markov dynamics, the connection between discrete-time and continuous-time Markov Chain Monte Carlo, simulation details, and additional results, which includes Refs. [46,47].
[46] A. B. Bortz, M. H. Kalos, and J. L. Lebowitz, J. Comput. Phys. **17**, 10 (1975).
[47] D. T. Gillespie, J. Phys. Chem. **81**, 2340 (1977).
[48] For a chain of N Ising spins, the number of states is $|\Omega| = 2^N$. For $|\Omega| = \infty$, the natural mathematical framework is functional analysis (rather than linear algebra).
[49] Superscripts b are twofold. They stress the fact that the observables $\mathcal{O}_k^b$ are tied to the bath temperature T_b, and that detailed balance, Eq. (4), is only fulfilled for the scalar product at temperature T_b.
[50] G. Parisi, *Statistical Field Theory* (Addison-Wesley, Reading, MA, 1988).
[51] Recall that $(\mathcal{M}_w^2)^\perp = \mathcal{M}_w^2 - \mathbf{1}\mathbb{E}^{T_b}[\mathcal{M}_w^2]$ mimics $\mathcal{O}_2^b$ in the sense that $\mathbb{E}^{T_b}[\mathcal{O}_2^b] = 0$. After accounting for normalization, $\alpha_2^{(t=0)} \approx \Lambda^{-1}\mathbb{E}^{T_b}[(\mathcal{M}_w^2)^\perp]$, which leads to Eq. (7).
[52] Strictly speaking, we computed the spectral decomposition of R using 300-digit arithmetic [45].
[53] S. Kullback and R. A. Leibler, Ann. Math. Stat. **22**, 79 (1951).
[54] A. Biswas, V. V. Prasad, and R. Rajesh, Phys. Rev. E **108**, 024902 (2023).
[55] A. Megías, A. Santos, and A. Prados, Phys. Rev. E **105**, 054140 (2022).
[56] L. B. Pires, R. Goerlich, A. L. da Fonseca, M. Debiossac, P.-A. Hervieux, G. Manfredi, and C. Genet, Phys. Rev. Lett. **131**, 097101 (2023).